ISSN 1061-9208, Russian Journal of Mathematical Physics, 2016, Vol. 23, No. 1, pp. 35–55. © Pleiades Publishing, Ltd., 2016.

Stokes–Leibenson Problem for Hele-Shaw Flow: a Critical Set in the Space of Contours

A. S. Demidov[*,**], **J.-P. Lohéac**[***,†], **and V. Runge**[****]

[*] *Lomonosov Moscow State University, Faculty of Mechanics and Mathematics; Leninskie gory, Moscow, 119899, Russia;*
[**] *Moscow Institute of Physics and Technology (State University), Dolgoprudny, Moscow Region, 141700, Russia,*
E-mail: demidov.alexandre@gmail.com
[***] *École Centrale de Lyon, Département Mathématiques et Informatique, Institut Camille-Jordan, (C.N.R.S. U.M.R. 5208), 36 avenue Guy-de-Collongue, 69134 ECULLY Cedex, France*
[****] *Université Paris-Dauphine, Centre De Recherche en Mathématiques de la Décision, Place du Maréchal De Lattre De Tassigny, 75775, Paris Cedex 16, France*
E-mail: vincent.runge@ceremade.dauphine.fr

Received December 28, 2015

Abstract. The Stokes–Leibenson problem for Hele-Shaw flow is reformulated as a Cauchy problem of a nonlinear integro-differential equation with respect to functions a and b, linked by the Hilbert transform. The function a expresses the evolution of the coefficient longitudinal strain of the free boundary and b is the evolution of the tangent tilt of this contour. These functions directly reflect changes of geometric characteristics of the free boundary of higher order than the evolution of the contour point obtained by the classical Galin–Kochina equation. That is why we managed to uncover the reason of the absence of solutions in the sink-case if the initial contour is not analytic at at least one point, to prove existence and uniqueness theorems, and also to reveal a certain critical set in the space of contours. This set contains one attractive point in the source-case corresponding to a circular contour centered at the source-point. The main object of this work is the analysis of the discrete model of the problem. This model, called quasi-contour, is formulated in terms of functions corresponding to a and b of our integro-differential equation. This quasi-contour model provides numerical experiments which confirm the theoretical properties mentioned above, especially the existence of a critical subset of co-dimension 1 in space of quasi-contours. This subset contains one attractive point in the source-case corresponding to a regular quasi-contour centered at the source-point. The main contribution of our quasi-contour model concerns the sink-case: numerical experiments show that the above subset is attractive. Furthermore, this discrete model allows to extend previous results obtained by using complex analysis. We also provide numerical experiments linked to fingering effects.

DOI 10.1134/S1061920816010039

This work is dedicated to the memory of our colleague and friend J.-P. LOHÉAC, who worked with us on this article.

1. INTRODUCTION

When presenting the first edition of the book [30], A. N. Krylov wrote in the preface: "Involuntarily, I remembered the spring session of the Marine Engineering Society in 1898. At this session, Prof. Hele-Shaw for the first time exhibited his cell, which was projected on a screen to show the streamlines of a jet flow past various kinds of obstacles." In the same 1898, Stokes [39] showed that the Hele-Shaw cell was (as Lamb wrote in [27]) "a beautiful experimental verification of the forms of streamlines for certain cases of stationary vortex-free planar motion."

The core of the Hele-Shaw device is a blob of fluid, for example, glycerin, moving between two glass plates. In recent decades, the attention of some scientists has been attracted to the problem of motion of such a blob when glycerin is injected or sucked through a small hole in one of the plates. The air that surrounds the blob is another fluid with negligible viscosity.

[†] Deceased.

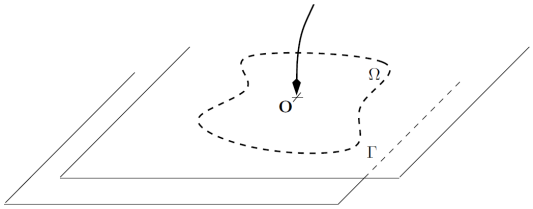

Fig. 1. Fluid is injected (or sucked) through some source-point (or sink-point) **O**.

In the idealization proposed by L. S. Leibenson [28], this viscosity vanishes. This corresponds to the case of constant pressure on the blob boundary. The classical statement of the Stokes-Leibenson problem for Hele-Shaw flows can be written as follows.

Let Ω_0 be a bounded simply connected domain in $\mathbb{R}^2$ enclosing the origin (where the source-sink point is located) and such that its boundary Γ_0 is smooth enough. This domain will be deformed according to the following law. At time t, we obtain a domain Ω_t with boundary Γ_t such that the normal velocity of each point $\mathbf{s}$ of Γ_t is given by

$$\textit{kinetic condition:} \qquad \dot{\mathbf{s}}.\nu = \partial_\nu u \quad \text{on } \Gamma_t\,,$$

where ν is the unit normal outward-pointing vector, $\partial_\nu u$ is the normal outside derivative of some real function u (see [28, 39]) defined in Ω_t by

$$\begin{array}{lll} \textit{Stokes equation for Hele-Shaw sell:} & \Delta u = q\delta & \text{in } \Omega_t\,, \\ \textit{Leibenson dynamical condition:} & u = 0 & \text{on } \Gamma_t\,. \end{array}$$

Here, $\Delta = \partial^2_{xx} + \partial^2_{yy}$ is the classical Laplace operator and δ is the " Dirac distribution" concentrated at the origin. The coefficient q belongs to $\mathbb{R}^*$ and characterizes the source-power (respectively, sink-power) when it is positive (respectively, negative).

Mathematical research about the above Stokes–Leibenson problem began with the papers of Galin [17] and Polubarinova–Kochina [33, 34], published in 1945. In these articles, the authors introduced a certain univalent mapping $f(\cdot,t)$ from the unit disk $\{\zeta \in \mathbb{C} \,/\, |\zeta| \leqslant 1\}$ onto the desired domain Ω_t and obtained the equation

$$2\pi\, \Re\left[\frac{\partial f}{\partial t}(\zeta,t)\,\overline{\left(\zeta\frac{\partial f}{\partial \zeta}\,(\zeta,t)\right)}\right] = q, \qquad |\zeta| = 1\,. \tag{1.1}$$

Under the assumption that $f(\zeta,t) = a_1(t) + a_2(t)\zeta + \cdots + a_n(t)\zeta^n$, Galin [17] obtained a system of ordinary differential equations for the coefficients $a_j(t)$. For $n = 2$, this system takes the form [34]

$$a_1^2(t)a_2(t) = a_1^2(0)a_2(0), \qquad a_1^2(t) + 2a_2^2(t) = a_1^2(0) + 2a_2^2(0) - \frac{qt}{\pi}\,.$$

If $|a_2/a_1| < 1/2$, then the image of the unit circle by the mapping $f(\cdot,t)$ is a limaçon Γ_0. In the sink case ($q < 0$), it is transformed in finite time into a cardioid Γ_{t_*} whose cusp does not reach the sink-point. Further (i.e., for $t > t_*$) the map $f(\cdot,t)$ stops being univalent and the solution $t \mapsto \Gamma_t$ ceases to exist. By using the meromorphic map $\zeta \mapsto f(\zeta,t)$, Kufarev [26] found a similar effect for a circle where the sink-point is shifted relatively to the center. The first theorem on the local solvability of the Stokes–Leibenson problem was obtained in [40].

In the last decades, such problems have often been called *problems of Hele-Shaw flows* or *Hele-Shaw free boundary problems* [31]. Interest in such problems increased in recent years (see, e.g., [18, 19, 21, 25, 29, 31] and references therein). These problems are also good models for some more complicated two-phases problems (see, e.g., [4, 5, 32]).

In this paper, we study the Stokes–Leibenson problem from a different point of view than the Galin–Kochina approach. Namely, applying the functional-geometric method [10], inspired by the

ideas of Helmholtz [22] and Kirchhoff [24], we reformulate the Stokes–Leibenson problem as a Cauchy problem for a nonlinear integro-differential equation. This is an equation with respect to two functions a and b linked by the Hilbert transform at each time $t \geqslant 0$. The function a expresses the evolution of the coefficient longitudinal strain of the free boundary and b is the evolution of the tangent tilt of this contour. These functions directly reflect changes in the geometric characteristics of the free boundary of order higher than that of the evolution of the contour point obtained by the classical Galin–Kochina equation. That is why we managed to uncover the reason of the absence of solutions in the sink-case, if the initial contour is not analytic at at least one point, to prove existence and uniqueness theorems for any $t > 0$ for a H^2-smooth initial contour close to the circle, and also to reveal a certain critical set in the space of contours. This set contains one attractive point in the source-case corresponding to a circular contour centered at the source-point.

This result was announced in [11], briefly outlined in the note [7] (see also [8, 9]). Furthermore, this leads to a discrete model, called *the quasi-contour model* [6, 14, 11, 12], which is very useful for obtaining qualitative properties. This allows us to present numerical results which show the existence of a critical subset, contained in $\mathfrak{M}$ and of co-dimension 1, in a fixed space of quasi-contours. The behavior near this subset can be an explanation of some physical instabilities.

In order to simplify some technical aspects, we shall rewrite the previous system, *the Stokes–Leibenson dynamical condition* in the following form:

(1) Ω_0 is a bounded simply connected domain in $\mathbb{R}^2$, symmetric with respect to the x-axis, containing the origin $\mathbf{O}$ (where the source-sink is located) such that its boundary Γ_0 is smooth enough;
(2) this domain will be deformed according to the following law: at time $t \geqslant 0$, one obtains a domain Ω_t of boundary Γ_t such that the normal velocity of almost every point $\mathbf{s}$ of Γ_t is given by following kinetic condition

$$\dot{\mathbf{s}}.\nu = \frac{q}{2}\,\partial_\nu u \qquad \text{on } \Gamma_t\,, \tag{1.2}$$

where the function u satisfies the following Stokes–Leibenson system

$$\begin{cases} \Delta u = 2\delta & \text{in } \Omega_t\,, \\ u = 0 & \text{on } \Gamma_t\,. \end{cases} \tag{1.3}$$

The proof of the equivalence with the above system, *the kinetic condition–Stokes equation–Leibenson dynamical condition* (see above) is immediate and is left to the reader.

It can be observed that the behavior of points of Γ_t depends on the shape of Ω_t through u and depends linearly on the flow-power q.

Our paper is organized in four following sections:

(1) *Geometrical transformation* [10]: techniques inspired by works of Helmholtz [22] and Kirchhoff [24].
(2) *Theoretical results*, concerning the Stokes–Leibenson problem.
(3) *Discrete problem*: an approximated Stokes–Leibenson problem and a numerical scheme, the so-called "*quasi-contour model*," are constructed there.
(4) *Numerical experiments*: some results obtained by using above model are given.

2. GEOMETRICAL TRANSFORMATION

In this Section, we consider a fixed bounded connected open set Ω of $\mathbb{R}^2$ with a conveniently regular boundary Γ so that a normal unit vector ν pointing outwards Ω and its directly orthogonal tangent unit vector τ can be defined almost everywhere. Furthermore, we suppose that Ω contains the origin point $\mathbf{O}$ of Cartesian coordinates and is symmetric with respect to the x-axis.

2.1. General Case

As above, we denote by δ the associated Dirac distribution.

Let us consider the following Laplace problem, similar to (1.3),

$$\begin{cases} \Delta u = 2\delta & \text{in } \Omega\,, \\ u = 0 & \text{on } \Gamma\,. \end{cases} \tag{2.1}$$

Let us now suppose that Ω is symmetric with respect to x-axis and define

$$\begin{aligned} \Omega^+ &= \{(x,y) \in \Omega \,/\, y > 0\}\,, \quad \Gamma^+ = \{(x,y) \in \Gamma \,/\, y > 0\}\,, \\ \gamma^- &= \{(x,0) \in \Omega \,/\, x < 0\}\,, \quad \gamma^+ = \{(x,0) \in \Omega \,/\, x > 0\}\,. \end{aligned}$$

Because of the symmetry with respect to the x-axis, the above problem (2.1) can be reduced to

$$\begin{cases} \Delta u = \delta & \text{in } \Omega^+\,, \\ u = 0 & \text{on } \Gamma^+\,, \\ \partial_\nu u = 0 & \text{on } \gamma^- \cup \gamma^+\,. \end{cases} \tag{2.2}$$

Then we can consider that u is a harmonic function in Ω^+ and introduce its harmonically conjugate function v such that the Cauchy–Riemann conditions are satisfied

$$\partial_x v = -\partial_y u \quad \text{and} \quad \partial_y v = \partial_x u \qquad \text{in } \Omega^+\,. \tag{2.3}$$

Remark 2.1. Since v is harmonically conjugate to u, we get $\nabla u.\nabla v = 0$ and $|\nabla v| = |\nabla u|$ in Ω^+ and $\nabla u = |\nabla u|\,\nu$ and $\nabla v = |\nabla v|\,\tau$ on Γ^+.

By using Green formula, one can easily get the following result.

Remark 2.2. γ^- and γ^+ are level curves for v and $\quad v_{|\gamma^-} - v_{|\gamma^+} = \displaystyle\int_{\Gamma^+} \partial_\nu u \, d\sigma = 1.$

Finally, without any constraint, we can choose v so that it satisfies

$$\begin{cases} \Delta v = 0 & \text{in } \Omega^+\,, \\ \partial_\nu v = 0 & \text{on } \Gamma^+\,, \\ v = 0 & \text{on } \gamma^+\,, \\ v = 1 & \text{on } \gamma^-\,. \end{cases} \tag{2.4}$$

Now let us now consider the analytic complex valued function $w = u + \imath v$ defined in Ω^+. By the maximum principle for harmonic functions, w is univalent from Ω^+ onto

$$\Pi = \{w = u + \imath v \,/\, (u,v) \in (-\infty, 0) \times (0,1)\}\,.$$

Since Π is simply connected, the Helmholtz–Kirchhoff function (see [10]) is well-defined in Π

$$A + \imath B = \ln \frac{dz}{dw}\,, \qquad \text{where } z(w) = x(u,v) + \imath y(u,v)\,, \tag{2.5}$$

where A and B are real-valued functions. By a continuity argument, we obtain $B(u,0) = 0$ and $B(u,1) = \pi$. Hence, the Helmholtz–Kirchhoff function can be written as follows:

$$A(u,v) + \imath B(u,v) = \alpha_0 + \pi(u + \imath v) + \sum_{k=1}^{\infty} \beta_k \exp\big(\pi k(u + \imath v)\big)\,, \tag{2.6}$$

where α_0 and β_k $(k \in \mathbb{N}^*)$ are real coefficients.

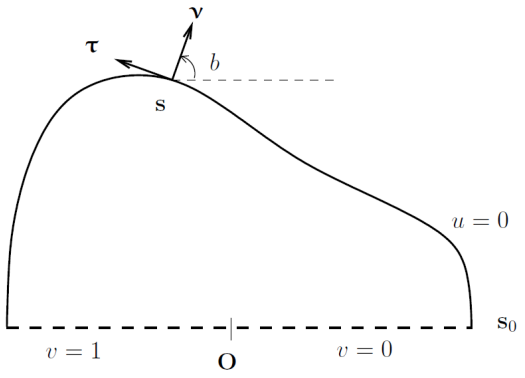

Fig. 2. Upper part of fluid domain.

Definition 2.1. From above formula, we can define *real functions* $\tilde{A}$, $\tilde{B}$, a, b, α, β such that

$$A(u,v) = \alpha_0 + \pi u + \tilde{A}(u,v)\,, B(u,v) = \pi v + \tilde{B}(u,v)\,,$$
$$\tilde{A}(u,v) = \sum_{k=1}^{\infty} \beta_k \exp(k\pi u)\cos(k\pi v), \quad \tilde{B}(u,v) = \sum_{k=1}^{\infty} \beta_k \exp(k\pi u)\sin(k\pi v)\,,$$
$$a(\eta) = A(0,\eta) = \alpha_0 + \alpha(\eta), \quad b(\eta) = B(0,\eta) = \pi\eta + \beta(\eta)\,,$$
$$\alpha(\eta) = \tilde{A}(0,\eta) = \sum_{k=1}^{\infty} \beta_k \cos(k\pi\eta), \quad \beta(\eta) = \tilde{B}(0,\eta) = \sum_{k=1}^{\infty} \beta_k \sin(k\pi\eta)\,.$$

Remark 2.3. Every point $z = x + \imath y$ of Ω^+ is linked to a unique point $w = u + \imath v$ of Π. Every point of Γ^+ is linked to a unique point $\eta \in (0,1)$ such that "$w = 0 + \imath\eta$."

Lemma 2.1. *The solution u of* (2.2) *and the solution v of* (2.4) *satisfy*

$$\nabla u = \exp(-A)\begin{pmatrix}\cos B\\ \sin B\end{pmatrix}, \quad \nabla v = \exp(-A)\begin{pmatrix}-\sin B\\ \cos B\end{pmatrix} \qquad \text{in } \overline{\Pi}\,.$$

Immediate consequences are

$$|\nabla u| = |\nabla v| = \exp(-A) \quad \text{in } \Pi \qquad \textit{and} \qquad |\nabla u| = |\nabla v| = \exp(-a) \quad \text{on } (0,1)\,.$$

Proof. From (2.5), we see that

$$\frac{dw}{dz} = \exp(-A - \imath B).$$

On the other hand, the Cauchy-Riemann conditions (2.3) yield

$$\frac{dw}{dz} = \partial_x u - \imath\partial_y u = \partial_y v + \imath\partial_x v.$$

Then the result can be deduced from (2.6).

Remark 2.4. A point $\mathbf{s} \in \Gamma^+$ is linked to the parameter $\eta \in (0,1)$, the normal and tangential unit vectors are given by

$$\nu = \begin{pmatrix}\cos b\\ \sin b\end{pmatrix}, \quad \tau = \begin{pmatrix}-\sin b\\ \cos b\end{pmatrix} \qquad \text{on } (0,1)\,,$$

and $\mathbf{s}$ is given by the following formula

$$\mathbf{s}(\eta) = \mathbf{s}_0 + \int_0^\eta \exp a(v)\,\tau(v)\,dv = \mathbf{s}_0 + e^{\alpha_0}\int_0^\eta \exp\alpha(v)\,\tau(v)\,dv\,, \qquad \text{with } \{\mathbf{s}_0\} = \overline{\Gamma^+} \cap \overline{\gamma^+}\,.$$

Remark 2.5. The measures of γ^+ (abscissa of $\mathbf{s}_0$), Γ^+ (dimension 1), and Ω^+ (dimension 2) are given by the following formulas:

$$|\gamma^+| = \int_{-\infty}^{0} \exp A(u,0)\,du = e^{\alpha_0} \int_{-\infty}^{0} \exp\bigl(\pi u + \tilde{A}(u,0)\bigr)\,du\,,$$
$$|\Gamma^+| = \int_{0}^{1} \exp a(v)\,dv = e^{\alpha_0} \int_{0}^{1} \exp \alpha(v)\,dv\,,$$
$$|\Omega^+| = \int_{\Pi} \exp 2A(u,v)\,du\,dv = e^{2\alpha_0} \int_{\Pi} \exp 2\bigl(\pi u + \tilde{A}(u,v)\bigr)\,du\,dv\,.$$

Let $b : \eta \mapsto b(\eta) = \pi\eta + \beta(\eta)$ be the angle between ν and the x-axis at the point $s(\eta) \in \Gamma^+$ and suppose that this function is regular enough so that

$$b(0) = 0\,, \qquad b(1) = \pi\,, \qquad \beta \in L^2(0,1)\,.$$

Then the Fourier expansion of β can be computed. The coefficient α_0 can be deduced from the formula for $|\Omega^+|$ in the previous Remark 2.5

$$\alpha_0 = \frac{1}{2}\,\ln|\Omega^+| - \frac{1}{2}\,\Upsilon(\tilde{\beta}) \qquad \text{with} \quad \Upsilon(\beta) = \ln\Bigl(\int_{\Pi} \exp 2\bigl(\pi u + \tilde{A}(u,v)\bigr)\,du\,dv\Bigr)\,. \tag{2.7}$$

This yields the functions a, A and the Helmholtz-Kirchhoff function by formula (2.5). Hence, the geometrical transformation from Π onto Ω^+ is known.

2.2. Circular Case

Remark 2.6. If $\beta = 0$, then Ω is a circular disk centered at $\mathbf{O}$ and the complex number $u + \imath v \in \Pi$ is linked to polar coordinates in the following sense:

$$r = \sqrt{2|\Omega^+|/\pi}\,\exp(\pi u)\,, \qquad \theta = \pi v\,.$$

2.3. Polygonal Case

A more interesting case concerns polygonal open sets. We consider the class $\mathcal{P}_m$ ($m \in \mathbb{N}^*$) of simply connected polygonal domains such that

(1) each of these domains is symmetric with respect to the x-axis and contains the origin;
(2) its boundary is a polygonal line with $2m$ vertices;
(3) consequently, $m-1$ edges belong to the half-plane $y > 0$.

Any such polygonal domain can be characterized by two sequences:

(1) the first one, $\sigma = (\sigma_0, \ldots, \sigma_m)$ satisfies $0 = \sigma_0 < \sigma_1 < \cdots < \sigma_{m-1} < \sigma_m = 1$; it gives the length of the edges; this sequence is defined by means of the function v harmonically conjugate to the solution u of problem (2.1) (see also (2.4)): σ_k is the value of v at the k-th vertex of the upper part of Γ^m;
(2) the second one, $\mathbf{N} = (N_1, \ldots, N_m)$, gives the orientation of edges, i.e., N_k is the angle between the x-axis and the normal unit vector pointing outwards Ω^m along the k-th edge of the upper part of Γ^m; because of the symmetry with respect to x-axis, we define $N_0 = -N_1$ and $N_{m+1} = 2\pi - N_m$.

The function b given in Definition 2.1 (and used in Remark 2.4) is piecewise constant:

$$\forall k \in \{1, \ldots, m\}\,, \quad \sigma_{k-1} < \eta < \sigma_k \implies b(\eta) = N_k\,. \tag{2.8}$$

Remark 2.7. The regular polygonal domain centered at the origin corresponds to the choice $\sigma = \widehat{\sigma}$ and $\mathbf{N} = \widehat{\mathbf{N}}$, where $\widehat{\sigma} = \Bigl(0, \frac{1}{m}, \ldots, \frac{m-1}{m}, 1\Bigr)$ and $\widehat{\mathbf{N}} = \Bigl(\frac{\pi}{2m}, \frac{3\pi}{2m}, \ldots, \frac{(2m-1)\pi}{2m}\Bigr)$.

Proposition 2.1. *If the function b is given by* (2.8)*, than the functions A and a will be*

$$\begin{aligned} A(u,v) &= \alpha_0 - \ln 2 - \frac{N_1}{\pi}\ln|\cosh\pi u - \cos\pi v| \\ &\quad - \frac{1}{2}\Big(1-\frac{N_m}{\pi}\Big)\ln\big|\big(\cosh\pi u - \cos\pi(v+1)\big)\big(\cosh\pi u - \cos\pi(v-1)\big)\big| \\ &\quad - \sum_{k=1}^{m}\frac{N_{k+1}-N_k}{2\pi}\ln\big|\big(\cosh\pi u - \cos\pi(v+\sigma_k)\big)\big(\cosh\pi u - \cos\pi(v-\sigma_k)\big)\big|\ , \\ a(\eta) &= \alpha_0 - \ln 2 - \frac{N_1}{\pi}\ln|1-\cos\pi\eta| - \Big(1-\frac{N_m}{\pi}\Big)\ln|\cos\pi\eta+1| \\ &\quad - \sum_{k=1}^{m}\frac{N_{k+1}-N_k}{\pi}\ln|\cos\pi\eta - \cos\pi\sigma_k|\ , \end{aligned}$$

where α_0 is given by (2.7)*.*

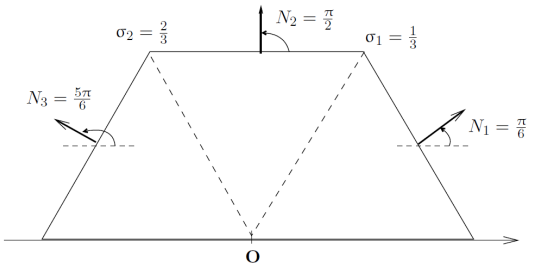

Fig. 3. Example of upper part of a centered regular hexagonal domain.

Proof. The classical Fourier expansion of β is

$$\beta(\eta) = \sum_{\jmath=1}^{\infty}\frac{2}{\jmath}\Big(\frac{N_1}{\pi} + \sum_{k=1}^{m}\frac{N_{k+1}-N_k}{\pi}\cos(\jmath\pi\sigma_k)\Big)\sin(\jmath\pi\eta)\,.$$

By Definition 2.1, we have

$$A(u,v) = \alpha_0 + \pi u + \sum_{\jmath=1}^{\infty}\beta_\jmath\exp(\jmath\pi u)\cos(\jmath\pi v).$$

We then get A from the following expansion, which holds for $u<0$ and $v\in(-1,1)$,

$$\sum_{\jmath=1}^{\infty}\frac{2}{\jmath}\exp(\jmath\pi u)\cos(\jmath\pi v) = -\ln 2 - \pi u - \ln|\cosh\pi u - \cos\pi v|\ .$$

For $v=\eta$, as $u\to 0$, the computation leads to the expansion of a.

Let us now introduce the following notation:

$$
\begin{aligned}
F_\jmath(u,v) &= \left|\frac{\big(\cosh\pi u-\cos\pi(v+\sigma_{\jmath-1})\big)\big(\cosh\pi u-\cos\pi(v-\sigma_{\jmath-1})\big)}{\big(\cosh\pi u-\cos\pi(v+\sigma_\jmath)\big)\big(\cosh\pi u-\cos\pi(v-\sigma_\jmath)\big)}\right|^{1/2}, \quad 1\leqslant\jmath\leqslant m\,,\\
F_{m+1}(u,v) &= \big|\big(\cosh\pi u-\cos\pi(v+1)\big)\big(\cosh\pi u-\cos\pi(v-1)\big)\big|^{1/2}\,,\\
G(\mathbf{N},u,v) &= 2\Big(\prod_{k=1}^{m}F_k(u,v)^{N_k/\pi}\Big)F_m(u,v)\,,\\
f_\jmath(\eta) &= F_\jmath(0,\eta)=\left|\frac{\sin\frac{\pi}{2}(\eta+\sigma_{\jmath-1})\,\sin\frac{\pi}{2}(\eta-\sigma_{\jmath-1})}{\sin\frac{\pi}{2}(\eta+\sigma_\jmath)\,\sin\frac{\pi}{2}(\eta-\sigma_\jmath)}\right|, \quad 1\leqslant\jmath\leqslant m\,, \qquad (2.9)\\
f_{m+1}(\eta) &= F_{m+1}(0,\eta)=2\left|\sin\frac{\pi}{2}(\eta+1)\,\sin\frac{\pi}{2}(\eta-1)\right|,\\
g(\mathbf{N},\eta) &= G(\mathbf{N},0,\eta)=2\Big(\prod_{k=1}^{m}f_k(\eta)^{N_k/\pi}\Big)f_m(\eta)\,.
\end{aligned}
$$

Proposition 2.2. *The notation* (2.9) *enables us to write*

$$
|\Omega^+|=e^{2\alpha_0}\int_\Pi\frac{1}{G(\mathbf{N},u,v)^2}\,du\,dv\,,\ |\gamma^+|=e^{\alpha_0}\int_{-\infty}^{0}\frac{1}{G(\mathbf{N},u,0)}\,du\,,\ \ |\Gamma^+|=e^{\alpha_0}\int_0^1\frac{1}{g(\mathbf{N},\eta)}\,d\eta\,.
$$

Proof. Proposition 2.1 and the notation (2.9) lead to

$$
A(u,v)=\alpha_0-\ln\big(G(\mathbf{N},u,v)\big)\,,\qquad a(\eta)=\alpha_0-\ln\big(g(\mathbf{N},\eta)\big)\,. \qquad (2.10)
$$

We obtain the result by using Remark 2.5.

3. THEORETICAL RESULTS

We now consider the Stokes–Leibenson problem (1.2), (1.3) mentioned in the Introduction. We here use the tools described in Section 2 in order to be able to constract a one parameter (t) chain of solutions (Ω_t,Γ_t). As we did in Section 2, we assume the existence of a fixed axis containing the point $\mathbf{O}$ with respect to which Ω_t and Γ_t are symmetric, and, at each time t, we shall use the above geometrical transformation in order to express u and find the kinetic behavior of the points of Γ_t^+. Hence, the functions given in Definition 2.1 depend on time t via the coefficient α_0 and the function β. In particular, we obtain

$$
\begin{aligned}
&a(t,\eta)=\alpha_0(t)+\alpha(t,\eta),\quad b(t,\eta)=\pi\eta+\beta(t,\eta),\\
&\alpha(t,\eta)=\sum_{k=1}^{\infty}\beta_k(t)\,\cos(k\pi\eta),\quad \beta(t,\eta)=\sum_{k=1}^{\infty}\beta_k(t)\,\sin(k\pi\eta).
\end{aligned} \qquad (3.1)
$$

Then we can observe that a point $\mathbf{s}$ of Γ_t^+ depends on time t and its position along Γ_t^+ depends on the parameter $\eta\in(0,1)$.

Proposition 3.1. *At each point of Γ_t^+, the normal velocity is independent of the parameter η.*

Proof. For any point $\mathbf{s}\in\Gamma_t^+$, we can write $\dot{\mathbf{s}}=\partial_t\mathbf{s}+\dot\eta\,\partial_\eta\mathbf{s}$, and observe that $\partial_\eta\mathbf{s}$ is a tangential vector to Γ_t^+ (see Remark 2.4). Taking the inner product by ν, we get normal velocity, $\dot{\mathbf{s}}.\nu=(\partial_t\mathbf{s}).\nu$, and this expression is independent of the choice of η.

3.1. Evolution Equation

Let us apply the results obtained in Section 2.

Proposition 3.2. *Assume that, at almost every point, Γ_t^+ is regular enough. Then, for $t > 0$ and $\eta \in (0,1)$,*

$$(e^a\,\partial_t b)\,(t,\eta) = \frac{q}{2}\left(e^{-a}\,\partial_\eta a\right)(t,\eta) + \partial_\eta b(t,\eta)\int_0^\eta \Big(e^a\,\partial_t a - \frac{q}{2}\,e^{-a}\,\partial_\eta b\Big)(t,v)\,dv\,.$$

Proof. Here we consider a point $\mathbf{s} = \mathbf{s}(t,\eta)$ that belongs to Γ_t^+. From (1.2), Remark 2.1, Lemma 2.1, and Proposition 3.1, we deduce $\dot{\mathbf{s}}.\nu = (\partial_t \mathbf{s}).\nu = q/2\,e^{-a}$. Taking the derivative with respect to η, we get, for $t > 0$ and $\eta \in (0,1)$,

$$(\partial^2_{\eta t}\mathbf{s}).\nu + (\partial_\eta b)\,(\partial_t \mathbf{s}).\tau = -(q/2)\,e^{-a}\,\partial_\eta a\,. \tag{3.2}$$

Using Remark 2.4, we obtain $\partial_\eta \mathbf{s} = e^a\,\tau$ and $\partial^2_{\eta t}\mathbf{s} = e^a\,((\partial_t a)\,\tau - (\partial_t b)\,\nu)$. Thus, $(\partial^2_{\eta t}\mathbf{s}).\nu = -e^a\,\partial_t b$ and $(\partial^2_{\eta t}\mathbf{s}).\tau = e^a\,\partial_t a$. Similarly, we compute

$$\partial_\eta\,((\partial_t \mathbf{s}).\tau) = (\partial^2_{\eta t}\mathbf{s}).\tau - (\partial_\eta b)\,(\partial_t \mathbf{s}).\nu = e^a\,\partial_t a - \frac{q}{2}\,e^{-a}\,\partial_\eta b\,.$$

Using the symmetry of the contour Γ with respect to the x-axis, we can write $(\partial_t \mathbf{s}).\tau = 0$ for $\eta = 0$. Then, for $t > 0$ and $\eta \in (0,1)$,

$$((\partial_t \mathbf{s}).\tau)\,(t,\eta) = \int_0^\eta \Big(e^a\,\partial_t a - \frac{q}{2}\,e^{-a}\,\partial_\eta b\Big)(t,v)\,dv\,. \tag{3.3}$$

Our result can now be easily deduced from (3.2), (3.3).

Corollary 3.1. *The above integro-differential equation can be written as follows*

$$\begin{aligned}
&\dot\beta(t,\eta) - \big((\pi + \partial_\eta\beta)\,e^{-\alpha}\big)(t,\eta)\int_0^\eta (\dot\alpha\,e^\alpha)(t,v)\,dv\\
&\quad = \frac{q}{2}e^{-2\alpha_0(t)}\Big[\big(\partial_\eta\alpha\,e^{-2\alpha}\big)(t,\eta) - \big((\pi + \partial_\eta\beta)\,e^{-\alpha}\big)(t,\eta)\int_0^\eta \big((\pi + \partial_\eta\beta)\,e^{-\alpha}\big)(t,v)\,dv\Big]\\
&\qquad + \dot\alpha_0(t)\Big[\big((\pi + \partial_\eta\beta)\,e^{-\alpha}\big)(t,\eta)\int_0^\eta e^{\alpha(t,v)}\,dv\Big].
\end{aligned}$$

Proof. We substitute formulas (3.1) into the equation of Proposition 3.2.

According to formulas (3.1) the functions α and β are linkedby the Hilbert transform. Having this in mind, let us write the integro-differentiable equation from Corollary 3.1 in the form

$$\big[\mathbb{I} + \mathbb{K}_0(\tilde\beta)\big]\,\dot{\tilde\beta} = \frac{q}{2}\,e^{-2\alpha_0}\,\mathbb{F}_1(\tilde\beta) + \dot\alpha_0\,\mathbb{F}_2(\tilde\beta)\,, \tag{3.4}$$

where $\mathbb{I}$ is the identity operator and

$$\mathbb{K}_0(\tilde\beta) : \dot\beta(t,\eta) \mapsto -\big((\pi + \partial_\eta\beta)\,e^{-\alpha}\big)(t,\eta)\int_0^\eta (\partial_t\alpha\,e^\alpha)(t,v)\,dv \tag{3.5}$$

$$\begin{aligned}
\mathbb{F}_1(\tilde\beta)(t,\eta) &= (\partial_\eta\alpha\,e^{-2\alpha})(t,\eta) - \big((\pi + \partial_\eta\beta)\,e^{-\alpha}\big)(t,\eta)\int_0^\eta \big((\pi + \partial_\eta\beta)\,e^{-\alpha}\big)(t,v)\,dv\,,\\
\mathbb{F}_2(\tilde\beta)(t,\eta) &= \big((\pi + \partial_\eta\beta)\,e^{-\alpha}\big)(t,\eta)\int_0^\eta e^{\alpha(t,v)}\,dv\,.
\end{aligned} \tag{3.6}$$

Proposition 3.3. *For all $t \geqslant 0$, the shape of Γ_t^+ is characterized by the Fourier coefficients of the function β.*

Proof. Observe that the rate of increase of the area of Ω_t is given by

$$\frac{d|\Omega_t|}{dt} = \int_{\Gamma_t} \dot{\mathbf{s}}.\nu \, d\gamma = \frac{q}{2} \int_{\Gamma_t} \partial_\nu u \, d\gamma = q \, .$$

In other words, $|\Omega_t^+| = \dfrac{q}{2}\, t + |\Omega_0^+|$. We now use Remark 2.5 to obtain the function α_0 and find A and a.

Using the function Υ given in (2.7), we can compute the coefficients depending on α_0 in equation (3.6)

$$e^{-2\alpha_0} = \frac{\exp(\Upsilon \circ \beta)}{|\Omega_t^+|} \quad \text{and} \quad \dot{\alpha}_0 = \frac{1}{2}\frac{d}{dt}\Big(\ln|\Omega_t^+| - \Upsilon \circ \beta\Big) \, . \tag{3.7}$$

Let us now define a new operator as follows

$$\mathbb{K}_1(\beta) : \dot{\tilde{\beta}} \longmapsto \Big[(t,\eta) \mapsto \frac{1}{2}\frac{d(\Upsilon \circ \tilde{\beta})}{dt}(t) \; \mathbb{F}_2(\tilde{\beta})(t,\eta)\Big]. \tag{3.8}$$

Theorem 3.1. *Consider problem* (1.2), (1.3). *If, Γ^+ is regular enough at almost every point, then the main unknown β satisfies the following integro-differential equation*

$$\big[\mathbb{I} + \mathbb{K}_0(\tilde{\beta}) + \mathbb{K}_1(\tilde{\beta})\big] \, \dot{\tilde{\beta}} = \frac{q}{|\Omega_t|} \, \Big[\exp\big(\Upsilon \circ \tilde{\beta}\big) \, \mathbb{F}_1(\tilde{\beta}) + \frac{1}{2} \, \mathbb{F}_2(\tilde{\beta})\Big], \tag{3.9}$$

where $\mathbb{K}_0$, $\mathbb{K}_1$, $\mathbb{F}_1$, $\mathbb{F}_2$, and Υ are, respectively, defined above in equations (3.4), (3.8), (3.5), (3.7) *and $|\Omega_t| = qt + |\Omega_0| \, , \forall t \geqslant 0$.*

Proof. Let us consider (3.6). From (3.7), we deduce the coefficient

$$\frac{q}{2}\, e^{-2\alpha_0(t)} = \frac{q}{qt + 2|\Omega_0^+|} \, \exp\big(\Upsilon(\tilde{\beta}(t))\big).$$

Again, from (3.7), we can deduce the time derivative of α_0,

$$\dot{\alpha}_0(t) = \frac{1}{2}\Big(\frac{q}{qt + 2|\Omega_0^+|} - \frac{\mathrm{d}(\Upsilon \circ \tilde{\beta})}{dt}(t)\Big) \, .$$

We finally rewrite (3.6) by using above formulas and (3.8).

Remark 3.1. The above formulas could be easily extended to the case of a time depending power flow. The corresponding law for fluid area should be

$$|\Omega_t^+| = \frac{1}{2}\int_0^t q(s) \, ds + |\Omega_0^+|.$$

3.2. Existence and Uniqueness Result

The case "$q = 2$ and $\tilde{\beta}$ small (in the sense of Fourier series)" has been studied by the above method in [8, 9]: it corresponds to a fluid domain close to a circle centered at the source-point.

Coordinatewise, the dynamical system (3.9) becomes

$$\left.\begin{array}{rcl} 2(t+t_0)\Big(\beta_1\dot{\beta}_1 + r_1(\beta)\dot{\beta}\Big) & = & \Big(-\beta_1^2 + 2\sum_{j\geqslant 2}\beta_j^2\Big) + s_1(\beta)\,, \\ 2(t+t_0)\Big(\dot{\beta}_k + r_k(\beta)\dot{\beta}\Big) & = & -(k+2)\beta_k + s_k(\beta) \qquad \text{for} \quad k\geqslant 2\,, \end{array}\right\} \tag{3.10}$$

where

$$|r_k(\beta)\dot{\beta}| \leqslant C\|\beta\|_1^{1+\mathrm{sgn}|k-1|}\|\dot{\beta}\|_0\,, \qquad |s_k(\beta)| \leqslant C\|\beta\|_1^{2+\mathrm{sgn}|k-1|}$$

and

$$\|\beta\|_1 = \max_t \sqrt{\sum_{k\geqslant 1}\Big(k\beta_k(t)\Big)^2}, \qquad \|\dot{\beta}\|_0 = \max_t \sqrt{\sum_{k\geqslant 1}\Big(\dot{\beta}_k(t)\Big)^2}.$$

Neglecting the terms containing r_j and s_j in (3.10), we obtain the system

$$\left\{\begin{array}{l} 2(t+|\Omega_0^+|)\bar{\beta}_1\dot{\bar{\beta}}_1 = -\bar{\beta}_1^2 + 2\displaystyle\sum_{j=2}^{\infty}\bar{\beta}_j^2\,, \\ 2(t+|\Omega_0^+|)\dot{\bar{\beta}}_k = -(k+2)\,\bar{\beta}_k\,, \quad \forall k\geqslant 2\,, \end{array}\right. \tag{3.11}$$

with respect to $\bar{\beta}(t,\eta) = \displaystyle\sum_{k\geqslant 1}\bar{\beta}_k(t)\,\sin(k\pi\eta)$.

Let us add the initial conditions

$$\bar{\beta}(0,\eta) = \beta(0,\eta) = \sum_{k\geqslant 1}\beta_k^0\sin(k\pi\eta)\,, \quad \eta\in(0,1)\,. \tag{3.12}$$

If initial data satisfy $\beta_1^0 \neq 0$, the solution of above Cauchy problem is

$$\left\{\begin{array}{c} \bar{\beta}_1(t) = \beta_1^0\Big(\frac{|\Omega_0^+|}{t+|\Omega_0^+|}\Big)^{1/2}\Big(1+\sum_{j=2}^{\infty}\frac{2}{j+1}\Big|\frac{\beta_j^0}{\beta_1^0}\Big|^2\Big(1-\Big(\frac{|\Omega_0^+|}{t+|\Omega_0^+|}\Big)^{j+1}\Big)\Big)^{1/2}, \\ \bar{\beta}_k(t) = \beta_k^0\Big(\frac{|\Omega_0^+|}{t+|\Omega_0^+|}\Big)^{1+k/2}\,, \quad \forall k\geqslant 2\,, \end{array}\right.$$

In [8, 9], it is proved that solution β of (3.9)–(3.12) behaves similarly to above function $\bar{\beta}$.

Theorem 3.2. *There exists a $C_* > 1$ such that for every (χ,ε,T) satisfying $\chi\geqslant 1$, $C_*\chi^3\varepsilon\leqslant 1$, $C_*\chi^2 T\leqslant 1$, and for initial data $\beta^0 : \eta\mapsto\beta^0(\eta) = \sum\limits_{k\geqslant 1}\beta_k^0\sin(k\pi\eta)$ belong to $H^1(0,1)$ and verifying*

$$|\beta_1^0| = \frac{\varepsilon}{8\chi}\,, \qquad \sum_{j\geqslant 2}k^2|\beta_j^0|^2 \leqslant \Big(\frac{\varepsilon}{8}\Big)^2\,,$$

problem (3.9)–(3.12) admits one and only one solution β belonging to some ε-neighborhood of zero in $\mathcal{C}(0,T;H^1(0,1))$. Furthermore, β can be approximated by $\bar{\beta}$, the solution of (3.11), (3.12), in the following sense

$$|\dot{\beta}_1(0) - \dot{\bar{\beta}}_1(0)| \leqslant C_*\varepsilon\,, \qquad \Big(\sum_{j\geqslant 2}|\dot{\beta}_j(0) - \dot{\bar{\beta}}_j(0)|^2\Big)^{1/2} \leqslant \chi\varepsilon\,.$$

This result shows, in particular, that the solution β of (3.9)–(3.12) follows from the solution $\bar{\beta}$ of (3.11), (3.12) under assumptions of Theorem 3.2. We can observe that the origin (with respect to β) is an attractive point when time increases. This means that the limit domain is circular and centered at the source point. Furthermore, the first equation in system (3.11) shows that the set "$\beta_1 = 0$" is critical in the sense that it does not give any solution. It can be observed that if, in the initial data, β_1 is small, then the speed $\dot{\beta}_1$, as well as $\dot{\bar{\beta}}_1$, is high. From these two remarks, we can deduce that locally the set "$\beta_1 = 0$" contains the origin which is attractive (when time increases) and that every other point of this set is repulsive (in the source case). This phenomena seems to be associated to the fact that the operator $\mathbb{I} + \mathbb{K}_0(\tilde{\beta}) + \mathbb{K}_1(\tilde{\beta})$ is singular. We shall try to develop a convenient numerical scheme in order to study the set

$$\mathfrak{M} = \{\tilde{\beta} \,/\, \mathbb{I} + \mathbb{K}_0(\tilde{\beta}) + \mathbb{K}_1(\tilde{\beta}) = 0\}\,. \tag{3.13}$$

Let us now complete this section with a global-in-time existence and uniqueness result.

Theorem 3.3. *There exists $\rho \in (0, 1/8)$ such that, for $\mu \in (0, 1]$, if the initial data β^0 belongs to $H^1(0,1)$ and satisfies*

$$0 < |\beta_1^0| \leqslant \mu\rho\,, \qquad \sum_{k=2}^{\infty} k^2 |\beta_k^0|^2 \leqslant (\mu\rho)^{1/2} |\beta_1^0|^{3/2}\,,$$

then problem (3.9)–(3.12) *admits one and only one solution $\beta \in \mathcal{C}(0, +\infty; H^1(0,1))$. If $\bar{\beta}$ is the reference function satisfying* (3.11), (3.12), *then*

$$|\dot{\beta}_1(0) - \dot{\bar{\beta}}_1(0)| \leqslant \mu\,, \qquad \Big(\sum_{k \geqslant 2} |\dot{\beta}_k(0) - \dot{\bar{\beta}}_k(0)|^2\Big)^{1/2} \leqslant \mu\,.$$

Furthermore, there exists some constant C slightly exceeding 1 *such that, for all $t \geqslant 0$, the following estimates hold*

$$|\dot{\beta}_1(t) - \dot{\bar{\beta}}_1(t)| \leqslant C\mu\,, \qquad \Big(\sum_{k \geqslant 2} |\dot{\beta}_k(t) - \dot{\bar{\beta}}_k(t)|^2\Big)^{1/2} \leqslant C\mu\,.$$

The reader can find a proof in [8, 9].

4. DISCRETE PROBLEM

We here try to develop a numerical method inspired by Euler's idea of "broken lines." To this end, we introduce a discrete model [6, 10] of problem (1.2), (1.3). The reader may also find some relationship with the Wulff crystal models from [1].

Our main idea has two aspects:

(1) we consider the class $\mathcal{P}_m$ ($m \in \mathbb{N}^*$) of simply connected polygonal domains (see Subsection 1.3);
(2) we compute the behavior of such domains, the so-called "quasi-contours," by applying a discrete law inspired by the law of motion of smooth curves in the classical Stokes–Leibenson problem.

4.1. Discrete Law and Notation

We fix a value of $m \in \mathbb{N}^*$ and consider polygonal domains belonging to $\mathcal{P}_m$. For such domains, we denote by $\tilde{\Gamma}_t^m$ the set of $2m$ vertices of the boundary Γ_t^m. At each point $\mathbf{p} \in \tilde{\Gamma}_t^m$, we define a quasi-normal unit vector pointing outwards from the domain, $\tilde{\nu}_{\mathbf{p}}$, and a quasi-tangential unit vector $\tilde{\tau}_{\mathbf{p}}$ (directly orthogonal with respect to $\tilde{\nu}_{\mathbf{p}}$). Further, we define a nonnegative weight function $d_{\mathbf{p}}$, which is positive at $\mathbf{p}$ and supported by the two edges around $\mathbf{p}$, so that the set of these weight functions is a partition of unity of Γ_t^m in the following sense: $\displaystyle\sum_{\mathbf{p} \in \tilde{\Gamma}_t^m} d_{\mathbf{p}} = 1\,,$ on Γ_t^m.

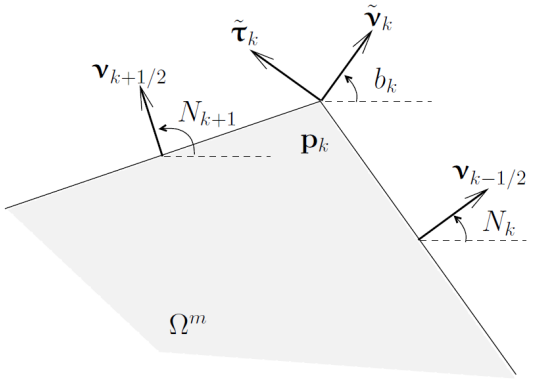

Fig. 4. Quasi-normal and quasi-tangent vectors at vertex $\mathbf{p}_k$.

We now consider a discrete problem close to the Stokes–Leibenson problem (1.2), (1.3). For $t \geqslant 0$, we want to construct Ω_t^m in $\mathcal{P}_m$, and its boundary Γ_t^m, so that for $t = 0$, Ω_0^m is given in $\mathcal{P}_m$ and all vertices of Γ_t^m verify the pointwise kinetic condition

$$\dot{\mathbf{p}}.\tilde{\nu}_{\mathbf{p}} = \frac{q}{2}\int_{\Gamma_t^m} d_{\mathbf{p}}\,|\nabla u|\,d\gamma\,, \quad \forall \mathbf{p} \in \tilde{\Gamma}_t^m\,, \tag{4.1}$$

where u satisfies (1.3) in Ω_t^m:

$$\begin{cases} \Delta u = 2\delta & \text{in } \Omega_t^m\,, \\ u = 0 & \text{on } \Gamma_t^m\,. \end{cases} \tag{4.2}$$

In order to build the numerical model, we use the tools introduced in Subsection 1.3: we consider a natural number $m \in \mathbb{N}^*$ and the first sequence σ as fixed parameters, which the second sequence $\mathbf{N}$ will be the main variable, depending on time. In particular, functions A and a depend on time through α_0 and $\mathbf{N}$ and, in this framework, using the functions G, g given by (2.9) and α_0 given by (2.7), formulas (2.10) can be rewritten as follows,

$$A(t,u,v) = \alpha_0(t) - \ln\big(G(\mathbf{N}(t),u,v)\big)\,, \qquad a(t,\eta) = \alpha_0(t) - \ln\big(g(\mathbf{N}(t),\eta)\big)\,.$$

For given parameters m and σ, we introduce some further notation:

(1) the $m+1$ vertices of the upper part of quasi-contour Γ^m: $\mathbf{p}_0, \mathbf{p}_1, \ldots, \mathbf{p}_m$ corresponding to sequence σ;
(2) the normal and tangential unit vectors along the edge $\mathbf{p}_k\mathbf{p}_{k+1}$: $\nu_{k+1/2}$ and $\tau_{k+1/2}$ (see (2.8));
(3) at each point $\mathbf{p}_k$, the quasi-normal and quasi-tangential unit vectors: $\tilde{\nu}_k$ and $\tilde{\tau}_k$, so that the speed of $\mathbf{p}_k$ is $\dot{\mathbf{p}}_k = R_k\tilde{\nu}_k + T_k\tilde{\tau}_k$, where R_k and T_k are quasi-normal and quasi-tangential speeds and

$$\tilde{\nu}_k = \begin{pmatrix} \cos b_k \\ \sin b_k \end{pmatrix}\,, \qquad \tilde{\tau}_k = \begin{pmatrix} -\sin b_k \\ \cos b_k \end{pmatrix}\,, \qquad \text{where } b_k = \frac{N_k + N_{k+1}}{2}\,.$$

Because of the symmetry, we have $T_0 = T_m = 0$. $T_1, \ldots, T_{m-1}$ are a priori unknown, as well as R_0, $R_1, \ldots, R_m$, which depend on t for a given parameter σ. The weight functions $d_{\mathbf{p}}$ in the kinetic condition (4.1) must be chosen so that the following properties hold

(**P1**) the pointwise kinetic condition (4.1) tends to the kinetic condition (1.2) as $m \to \infty$,

(**P2**) for a regular quasi-contour centered at the origin (see Remark 2.7), we must have:

$$R_0 = R_1 = \cdots = R_m\,.$$

To this end, we make the following elementary choice: we first introduce the sequence

$$\lambda_k = \frac{\sigma_{k-1}+\sigma_k}{2}\,,\ \text{if}\ \ 1 \leqslant k \leqslant m\,;\ \ \lambda_0 = -\lambda_1\,;\ \ \lambda_{m+1} = 2-\lambda_m\,;$$

we then define the k-th weight function by using the characteristic function χ_k of $(\lambda_k, \lambda_{k+1})$,

$$d_{\mathbf{p}_k} = \frac{1}{\lambda_{k+1}-\lambda_k}\,\chi_k\,.$$

Lemma 4.1. *Under above choice, the kinetic condition* (4.1) *at each vertex* $\mathbf{p}_k$ $(0 \leqslant k \leqslant m)$ *can be written as*

$$R_k = \frac{q}{2}\,\exp(-\alpha_0)\,\rho_k(\mathbf{N})\,, \qquad \text{with}\ \ \rho_k(\mathbf{N}) = \frac{1}{\lambda_{k+1}-\lambda_k}\int_{\lambda_k}^{\lambda_{k+1}} g(\mathbf{N},\eta)\,d\eta\,.$$

Proof. We use Lemma 2.1, formula (2.10) and the notation introduced above.

4.2. Discrete Model

We are now able to give a discrete version of equation (3.6) from Section 3. The following result is very useful for the construction of a convenient numerical scheme.

Theorem 4.1. *Let* $m \in \mathbb{N}^*$ *and* σ *be fixed parameters as above. If* (Ω_t^m, Γ_t^m) *is solution of the discrete Stokes–Leibenson problem* (4.1), (4.2), *then the associated functions* $t \longmapsto \alpha_0(t)$ *and* $t \longmapsto \mathbf{N}(t)$ *satisfy the equation*

$$Q_0(\mathbf{N})\dot{\mathbf{N}} = \frac{q}{2}\,e^{-2\alpha_0}\,P^0(\mathbf{N}) + \dot{\alpha}_0\,P^1(\mathbf{N})\,,$$

where $Q_0 = (q_{kj})_{1\leqslant k,j\leqslant m}$, $P^0 = (p_k^0)_{1\leqslant k\leqslant m}$ *and* $P^1 = (p_k^1)_{1\leqslant k\leqslant m}$ *can be expressed via the functions* f_j, g *given by* (2.9) *and* ρ_j *given in Lemma* 4.1, *in the following way* (δ_{kj} *is the classical Kronecker symbol*),

$$\begin{aligned}
q_{kj}(\mathbf{N}) = {}& \frac{1}{\pi}\left[\tan\frac{N_k-N_{k-1}}{2}\int_0^{\sigma_{k-1}}\frac{\ln f_j(\eta)}{g(\mathbf{N},\eta)}\,d\eta + \tan\frac{N_{k+1}-N_k}{2}\int_0^{\sigma_k}\frac{\ln f_j(\eta)}{g(\mathbf{N},\eta)}\,d\eta\right] \\
& + \delta_{kj}\int_{\sigma_{k-1}}^{\sigma_k}\frac{d\eta}{g(\mathbf{N},\eta)}\,, \\
p_k^0(\mathbf{N}) = {}& \rho_{k-1}(\mathbf{N})\cos\frac{N_k-N_{k-1}}{2} - \rho_k(\mathbf{N})\cos\frac{N_{k+1}-N_k}{2} \\
& + (\delta_{k1}-1)\,\tan\frac{N_k-N_{k-1}}{2}\sum_{j=1}^{k-1}\left[\rho_{j-1}(\mathbf{N})\sin\frac{N_j-N_{j-1}}{2} + \rho_j(\mathbf{N})\sin\frac{N_{j+1}-N_j}{2}\right] \\
& - \tan\frac{N_{k+1}-N_k}{2}\sum_{j=1}^{k}\left[\rho_{j-1}(\mathbf{N})\sin\frac{N_j-N_{j-1}}{2} + \rho_j(\mathbf{N})\sin\frac{N_{j+1}-N_j}{2}\right], \\
p_k^1(\mathbf{N}) = {}& \tan\frac{N_k-N_{k-1}}{2}\int_0^{\sigma_{k-1}}\frac{d\eta}{g(\mathbf{N},\eta)} + \tan\frac{N_{k+1}-N_k}{2}\int_0^{\sigma_k}\frac{d\eta}{g(\mathbf{N},\eta)}\,.
\end{aligned}$$

Proof. With the above notation, for $t > 0$ we can write

$$\mathbf{p}_{k+1} - \mathbf{p}_k = \int_{\sigma_k}^{\sigma_{k+1}} e^a\tau_{k+1/2}\,d\eta = \left(\int_{\sigma_k}^{\sigma_{k+1}} e^a\,d\eta\right)\tau_{k+1/2}\,.$$

Differentiating with respect to t, we obtain

$$\dot{\mathbf{p}}_{k+1} - \dot{\mathbf{p}}_k = \left(\int_{\sigma_k}^{\sigma_{k+1}} e^a \, \partial_t a \, d\eta \right) \tau_{k+1/2} - \dot{N}_{k+1} \left(\int_{\sigma_k}^{\sigma_{k+1}} e^a \, d\eta \right) \nu_{k+1/2} \,. \tag{4.3}$$

But we have

$$\dot{\mathbf{p}}_{k+1} - \dot{\mathbf{p}}_k = R_{k+1}\tilde{\nu}_{k+1} + T_{k+1}\tilde{\tau}_{k+1} - R_k\tilde{\nu}_k - T_k\tilde{\tau}_k \,. \tag{4.4}$$

One can easily observe

$$\tilde{\nu}_k.\nu_{k+1/2} = \tilde{\tau}_k.\tau_{k+1/2} = \cos\frac{N_{k+1}-N_k}{2}\,, \quad \tilde{\nu}_{k+1}.\nu_{k+1/2} = \tilde{\tau}_{k+1}.\tau_{k+1/2} = \cos\frac{N_{k+2}-N_{k+1}}{2}\,,$$
$$\tilde{\nu}_k.\tau_{k+1/2} = -\tilde{\tau}_k.\nu_{k+1/2} = -\sin\frac{N_{k+1}-N_k}{2}\,, \quad \tilde{\nu}_{k+1}.\tau_{k+1/2} = -\tilde{\tau}_{k+1}.\nu_{k+1/2} = \sin\frac{N_{k+2}-N_{k+1}}{2}\,.$$

Now, with (4.3) and (4.4), we compute $(\dot{\mathbf{p}}_{k+1} - \dot{\mathbf{p}}_k).\tau_{k+1/2}$, $(\dot{\mathbf{p}}_{k+1} - \dot{\mathbf{p}}_k).\nu_{k+1/2}$,

$$\begin{aligned} \int_{\sigma_k}^{\sigma_{k+1}} e^a \, \partial_t a \, d\eta \;&= R_{k+1}\sin\frac{N_{k+2}-N_{k+1}}{2} + R_k\sin\frac{N_{k+1}-N_k}{2} \\ &\quad + T_{k+1}\cos\frac{N_{k+2}-N_{k+1}}{2} - T_k\cos\frac{N_{k+1}-N_k}{2}\,, \end{aligned} \tag{4.5}$$

$$\begin{aligned} \left(\int_{\sigma_k}^{\sigma_{k+1}} e^a \, d\eta \right) \dot{N}_{k+1} = &-R_{k+1}\cos\frac{N_{k+2}-N_{k+1}}{2} + R_k\cos\frac{N_{k+1}-N_k}{2} \\ &+ T_{k+1}\sin\frac{N_{k+2}-N_{k+1}}{2} + T_k\sin\frac{N_{k+1}-N_k}{2}\,. \end{aligned} \tag{4.6}$$

Summing the above equations (4.5) from $k = 0$ to $k = \jmath - 1$ ($\jmath \in \mathbb{N}^*$, $\jmath < m+1$) and taking into account the fact that $T_0 = 0$, we obtain

$$T_\jmath \cos\frac{N_{\jmath+1}-N_\jmath}{2} = \int_0^{\sigma_\jmath} e^a \, \partial_t a \, d\eta - \sum_{k=0}^{\jmath-1} \left[R_{k+1}\sin\frac{N_{k+2}-N_{k+1}}{2} + R_k\sin\frac{N_{k+1}-N_k}{2} \right] .$$

This gives $T_\jmath$. We substitute this expression into (4.6). From formulas (2.9) and (2.10), we deduce

$$a(t,\eta) = \alpha_0(t) - \ln g(\mathbf{N}(t),\eta)\,, \qquad \partial_t a(t,\eta) = \dot{\alpha}_0(t) - \frac{1}{\pi}\sum_{\jmath=1}^{m} \dot{N}_\jmath(t)\ln f_\jmath(\eta)\,.$$

Using Lemma 4.1, we finally get the required differential equation.

Remark 4.1. Since the domain Ω_t is assumed connected, the vector-function $\mathbf{N}$ satisfies

$$\begin{cases} -\dfrac{\pi}{2} < N_1 < \dfrac{\pi}{2}\,, \\ -\pi < N_k - N_{k-1} < \pi\,, \quad \forall k \in \{2,\dots,m\}\,, \\ \dfrac{\pi}{2} < N_m < \dfrac{3\pi}{2}\,. \end{cases} \tag{4.7}$$

These conditions give the existence of every integral term in formulas introduced in Proposition 2.2 and Theorem 4.1.

This leads us to define a set of constraints about the sequences $\mathbf{N}$.

Definition 4.1. For given $m \in \mathbb{N}^*$, the set of constraints, $\mathfrak{U}_m$ is the set of sequences $\mathbf{N} \in \mathbb{R}^m$ such that (4.7) is satisfied and the generating vertices $\mathbf{p}_1, \dots, \mathbf{p}_{m-1}$ have a nonnegative second coordinate.

Theorem 4.2. *The equation of the previous theorem can be simplified and transformed into a Cauchy problem. Using the same notation as in Theorem* (4.1)*, we obtain the equation*

$$Q(\mathbf{N})\dot{\mathbf{N}} = \frac{q}{2}\, e^{-2\alpha_0} \left(P^0(\mathbf{N}) + \frac{1}{2|\omega|}\, P^1(\mathbf{N}) \right),$$

where $Q(\mathbf{N}) = Q_0(\mathbf{N}) + Q_1(\mathbf{N})$. $\overline{Q}(\mathbf{N})$ *verifies the equality*

$$Q_1(\mathbf{N})\,\dot{\mathbf{N}} = \frac{1}{2|\omega|}\frac{d|\omega|}{dt}\, P^1(\mathbf{N}) \quad \textit{with } |\omega| = \frac{1}{2} \sum_{0\leqslant k<i\leqslant m-1} \sin(N_{i+1}-N_{k+1}) \int_{\sigma_k}^{\sigma_{k+1}} \frac{1}{g(\eta)}\, d\eta \int_{\sigma_i}^{\sigma_{i+1}} \frac{1}{g(\eta)}\, d\eta,$$

$$\begin{aligned}\frac{d|\omega|}{dt} = {} & \frac{1}{2} \sum_{0\leqslant k<i\leqslant m-1} (\dot{N}_{i+1} - \dot{N}_{k+1}) \cos(N_{i+1} - N_{k+1}) \int_{\sigma_k}^{\sigma_{k+1}} \frac{1}{g(\eta)}\, d\eta \int_{\sigma_i}^{\sigma_{i+1}} \frac{1}{g(\eta)}\, d\eta \\ & + \frac{1}{2} \sum_{0\leqslant k<i\leqslant m-1} \sum_{n=1}^{m} \frac{\dot{N}_n}{\pi} \left[\int_{\sigma_k}^{\sigma_{k+1}} \frac{\ln f_n(\eta)}{g(\eta)}\, d\eta \int_{\sigma_i}^{\sigma_{i+1}} \frac{1}{g(\eta)}\, dv \right. \\ & \left. + \int_{\sigma_k}^{\sigma_{k+1}} \frac{1}{g(v)}\, d\eta \int_{\sigma_i}^{\sigma_{i+1}} \frac{\ln f_n(\eta)}{g(\eta)}\, d\eta \right] \sin(N_{i+1} - N_{k+1}).\end{aligned}$$

Proof. The area of the fluid delimited by the quasi-contour is a polygon, and this area can be expressed by the following formula $|\Omega| = \frac{1}{2}\sum_{i=0}^{m-1}(x_i y_{i+1} - x_{i+1} y_i)$, where (x_i, y_i) are the coordinates of the i-th vertex. We already know that

$$x_i = \left(|\gamma_0| - \sum_{k=1}^{i} \sin\, N_k \int_{\sigma_{k-1}}^{\sigma_k} \frac{1}{g(v)}\, dv \right) e^{\alpha_0}, \quad y_i = \left(\sum_{k=1}^{i} \cos\, N_k \int_{\sigma_{k-1}}^{\sigma_k} \frac{1}{g(v)}\, dv \right) e^{\alpha_0};$$

by introducing the notation $x_{i+1} = (\tilde{x}_i - s_i)e^{\alpha_0}$ and $y_{i+1} = (\tilde{y}_i + c_i)e^{\alpha_0}$, we immediately obtain

$$|\Omega| = e^{2\alpha_0}|\omega| = \frac{1}{2} e^{2\alpha_0} \sum_{i=0}^{m-1} (\tilde{x}_i c_i + \tilde{y}_i s_i)\,. \tag{4.8}$$

Remembering that the m-th vertex belongs to the x-axis, we deduce the relation

$$\sum_{i=0}^{m-1} \cos\, N_{i+1} \int_{\sigma_i}^{\sigma_{i+1}} \frac{1}{g(v)}\, dv = 0\,,$$

and a direct calculation of the area using the above expressions leads to the result for $|\omega|$. Differentiating the first equality in (4.8) and using the expression $\frac{d|\Omega|}{dt} = \frac{q}{2}$, we succeed to remove $\dot{\alpha_0}$ in the equation.

4.3. Numerical Scheme

We implement an explicit Euler scheme with respect to time. The originality in our method consists in the choice of the time scale, which is not a chosen parameter, but a consequence of constraint on the angles. Supposing that the sequences $\left(\mathbf{N}^0, \mathbf{N}^1, \ldots, \mathbf{N}^\ell\right)$ and $\left(\alpha_0^0, \alpha_0^1, \ldots, \alpha_0^\ell\right)$ are known for successive times $t_0 = 0$, t_1, …, t_ℓ, then we compute $\mathbf{N}^{\ell+1}$ and $\alpha_0^{\ell+1}$ at time $t_{\ell+1} > t_\ell$ by the following formulas

$$\begin{cases} \dfrac{\mathbf{N}^{\ell+1} - \mathbf{N}^\ell}{t_{\ell+1} - t_\ell} = \dfrac{q}{2}\, \exp(-2\alpha_0^\ell)\, Q(\mathbf{N}^\ell)^{-1} \left(P^0(\mathbf{N}) + \dfrac{1}{2|\omega|}\, P^1(\mathbf{N}) \right), \\ \alpha_0^{\ell+1} = \dfrac{1}{2} \ln \dfrac{|\Omega|(\mathbf{N}^{\ell+1})}{|\omega|(\mathbf{N}^{\ell+1})}\,. \end{cases} \tag{4.9}$$

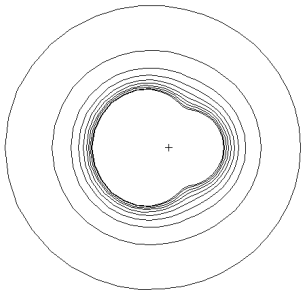

Fig. 5. Evolution in time of a quasi-contour in the source-case.

To avoid fast movement of the boundary, we chose to fix the quantity $\max_{i=1,\dots,m} |\mathbf{N}_i{}^{\ell+1} - \mathbf{N}_i{}^{\ell}|$ to be a constant C. The value $t_{\ell+1} - t_\ell$ is therefore equals to $C/\max_{i=1,\dots,m} |\mathbf{N}_i{}^{\ell+1} - \mathbf{N}_i{}^{\ell}|$. The variation of the area (and time) is then a consequence of this previous choice

$$\frac{d|\Omega|}{|\Omega|} = \frac{q\,C}{e^{2\alpha_0}|\omega| \max_{i=1,\dots,m} \dot{N}_i}\,.$$

The expression for $\alpha_0^{\ell+1}$ in (4.9) is explicitly found using the formulas in Theorem 4.2.

The main difficulty of this scheme is that, for some ℓ, $\det\big(Q(\mathbf{N}^\ell)\big)$ can be close to 0.

In this case, an iterative method is used in order to avoid the calculation of Q^{-1}.

Before giving numerical results, we define the critical subset of codimension 1 which corresponds to a discrete version of (3.13). Of course, it depends on parameter σ via the matrix $\tilde{Q}(\mathbf{N})$ (see the beginning of Subsection 4.1).

Definition 4.2. For given $m \in \mathbb{N}^*$ and fixed parameters σ, the *critical subset* is

$$\mathfrak{M}_m = \{\mathbf{N} \in \mathfrak{U}_m \,/\, \det\big(Q(\mathbf{N})\big) = 0\,\}\,.$$

This discrete model set $\mathfrak{M}_m$ is an analog of the set $\mathfrak{M}$ given by (3.13)

5. NUMERICAL EXPERIMENTS

In our program implemented in C++, we chose the same initial conditions for all examples. We fixed $|\Omega_0| = 100$, $q = \pm 1$ and $C = 2$. In all cases, we looked at the evolution of $\det\big(\tilde{Q}(\mathbf{N})\big)$ and visually compared the numerical results with exact solutions.

Initial conditions for $\mathbf{N}$ are a discretization of the graphical representation of an analytic function $z = f(\zeta)$ with $|\zeta| = 1$. The sequence σ is found using a software specialized in finite element calculation (FreeFem++).

5.1. Source-Case

Our aim is to verify that, in the source-case, quasi-contours usually tend to regular centered ones for initial contours near to a regular polygon.

Here the initial contour is the 20 edge discretization of the curve $z = \zeta - 0.2\zeta^2 + 0.2\zeta^3$ with $|\zeta| = 1$. In order to understand how the quasi-contour evolves, we define:

$$\rho = \frac{\max\{\mathbf{Op}_k / 0 \leqslant k \leqslant m\}}{\min\{\mathbf{Op}_k / 0 \leqslant k \leqslant m\}}\,.$$

In Fig. 5, we present the evolution in time of the initial configuration with nine other shapes, the last one been the 38th iteration. The source-point, represented by the cross, with power ($q = 1$), guaranteed that time and area evolve at the same speed.

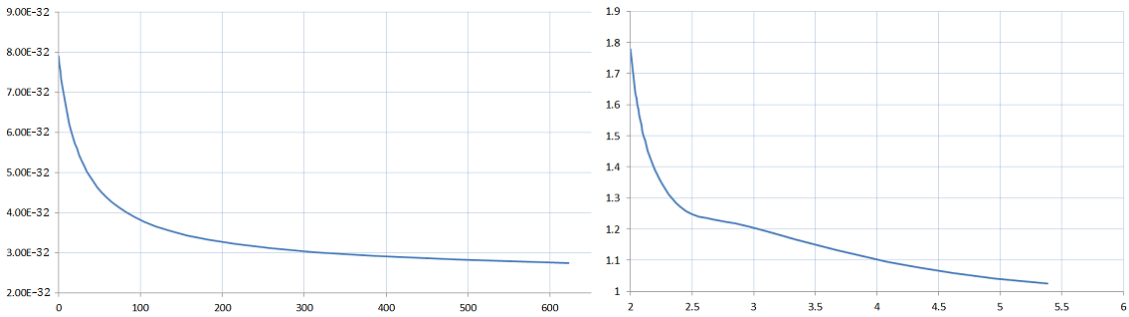

Fig. 6. Evolution in time of the determinant of the matrix Q as a function of time (left) and of ρ as a function of $\log(|\Omega|)$ (right).

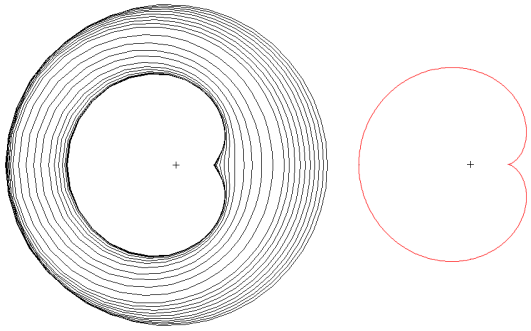

Fig. 7. Evolution in time in the sink-case of a quasi-contour leading to a cardioid.

The determinant of the matrix Q (left side) and the value of ρ (right side) are given on next Fig. 6; they are functions of time and $\log(|\Omega|)$, respectively.

We observed that the chosen quasi-contour tends to a regular one, which belongs to the critical subset $\mathfrak{M}_{15}$. The attractivity is very slow when time increases. This confirms that the circular contour (for initial contour 'near' to a regular polygon) is the limit of contour when $t \longrightarrow +\infty$, in the source-case. We have proceeded to many other numerical experiments (different geometrical cases and higher values of m) and obtained similar behaviors which confirm the theoretical results given in Section 3.

5.2. Sink-Case

To underline the efficiency of our method, we chose to numerically reproduce the evolution of well-known exact solutions.

Classical Galin–Kochina example : cardioid case. Fig. 7 represents the evolution in time of a quasi-contour (left side), whose initial shape is the 20 edge discretization of the graphical representation $z = \zeta - 0.05\zeta^2\,, |\zeta| = 1$. We observed that the obtained quasi-contour came closer to a cardioid (the exact solution) when $\det\big(Q(\mathbf{N})\big)$ approached zero. For comparison, we gave the exact solution (right side).

We notice that the calculation can go further until the domain remains connected. As observed in Fig. 8, the determinant moves away from zero after the occurrence of a cusp. This also gives us a way to understand numerically when the quasi-contour is the best discretization of the final exact solution (contour with a cusp).

Higher symmetry case. We also give examples of more complicated behavior which correspond to a higher symmetry configuration. The discretization is that of a corner domain, i.e., an infinite angle $\alpha < \pi$. The numerical scheme remains explicit with small modifications in formulas. Explanations can be found in [13].

We consider three initial 10-edge quasi-contours, whose edges are deduced from following graphical representations : $z = \zeta - 0.02\zeta^3\,, |\zeta| = 1$ (a) ; $z = \zeta - 0.02\zeta^4\,, |\zeta| = 1$ (b) and; $z = \zeta - 0.01\zeta^7$, $|\zeta| = 1$ (c).

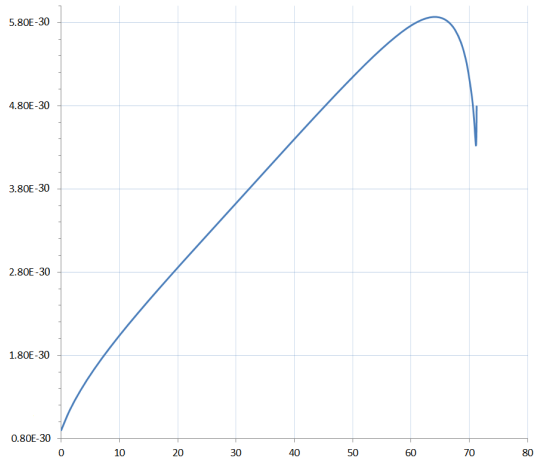

Fig. 8. Evolution in time of the determinant of the matrix Q.

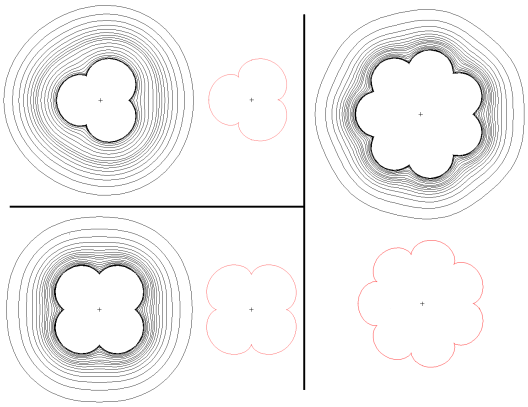

Fig. 9. Evolution in time of quasi-contours in the sink-case, and exact solutions for (a) (left side up), (b) (left side bottom) and (c) (right side).

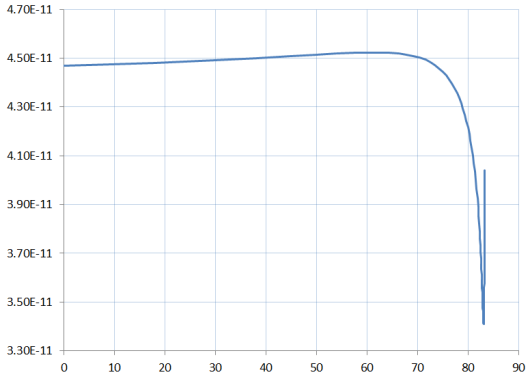

Fig. 10. Evolution in time of $\det\big(Q(\mathbf{N})\big)$ for the quasi-contour (a).

We present results in Fig. 9, giving for each time evolution the exact solution.

Again, we conclude that the moment when cusps occur corresponds to a minimum of function $\det\big(Q(\mathbf{N})\big)$. For example, in Fig. 10 we represent the time evolution of $\det\big(Q(\mathbf{N})\big)$ for the quasi-contour (a).

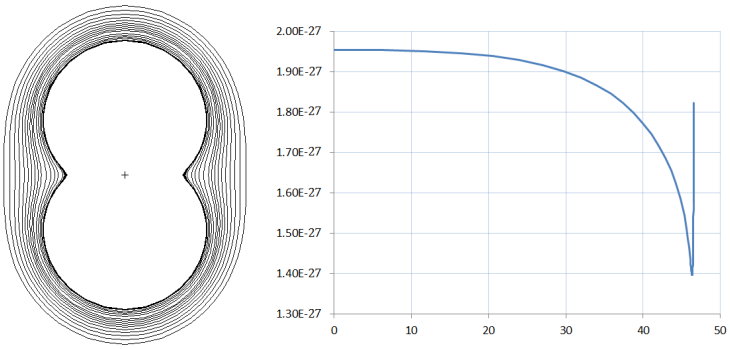

Fig. 11. Evolution in time of quasi-contour (left side) and his determinant $\det\big(Q(\mathbf{N})\big)$ (right side).

We have tried to reproduce the evolution of a more complicated solution. In [20], we consider an initial contour leading, when first cusp occurs, to the superposition of two identical circles, whose sink-point is located at the unique intersection.

In Fig. 11, we represented the time evolution of the 20-edge initial quasi-contour until the cusp occurs (left side) and the function $\det\big(Q(\mathbf{N})\big)$ depending on time (right side).

The conclusion concerning the determinant remains the same, however, the final quasi-contour does not draw two circles. The loss in accuracy certainly comes to the low number of edges chosen for the discretization. Another explanation could be the choice of the parameter C, whose value should be smaller to improve results.

We managed to construct a scheme that demonstrates a high accuracy in numerical results. Further work on the convergence of the numerical scheme must be done, since a Cauchy problem has be found.

ACKNOWLEDGEMENTS

The authors gratefully acknowledge CNRS (project “EDC25172”), region Rhône–Alpes (project “CIBLE 2010”) and the Russian Foundation for Basic Research (project 16-01-00781) for providing financial support for this scientific collaboration.

REFERENCES

1. R. Almgren, “Crystalline Saffman–Taylor Fingers,” SIAM J. Appl. Math. **55**, 1511–1535 (1995).
2. A. Antontsev, A. M. Meirmanov, and V. Yurinsky, *Hele-Shaw Flow in Two Dimensions: Global-In-Time Classical Solutions* (Universidade da Beira Interior, Portugal, preprint **6**, 1999).
3. B. V. Bazaliĭ, “On a Proof of the Classical Solvability of the Hele-Shaw Problem with a Free Boundary,” Ukrainian Math. J. **50** (11), 1452–1462 (1998).
4. G. Caginalp, “Stefan and Hele-Shaw Type Models as Asymptotic Limits of the Phase-Field Equations,” Phys. Rev. A **39** (11), 5887–5896 (1989).
5. G. Caginalp and X. Chen, “Convergence of the Phase Field Model to Its Sharp Interface Limits,” European J. Appl. Math. **9** (4), 417–445 (1998).
6. A. S. Demidov, “A Polygonal Model for the Hele-Shaw Flow,” Uspekhi Mat. Nauk. **4**, 195–196 (1998).
7. A. S. Demidov, “On Evolution of a Small Perturbation of a Circle in a Problem for Hele-Shaw Flows,” Russian Math. Surveys **57** (6), 1212-1214 (2002).
8. A. S. Demidov, “Evolution of the Perturbation of a Circle in the Stokes–Leibenson Problem for a Hele-Shaw Flow,” Sovrem. Mat. Prilozh. No. 2, Differ. Uravn. Chast. Proizvod. (2003), 3–24 [J. Math. Sci. (N. Y.) **123** (5), 4381–4403 (2004)].
9. A. S. Demidov, “Evolution of the Perturbation of a Circle in the Stokes–Leibenson Problem for a Hele-Shaw Flow. II,” Sovrem. Mat. Prilozh. No. 24, Din. Sist. i Optim. (2005), 51–65 [J. Math. Sci. (N. Y.) **139** (6), 7064–7078 (2006)].
10. A. S. Demidov, “A Functional-Geometric Method for Solving Problems with a Free Boundary for Harmonic Functions,” Uspekhi Mat. Nauk **65** (1), 3–96 (2010) [Russian Math. Surveys **65** (1), 1–94 (2010)].
11. A. S. Demidov and J.-P. Lohéac, “The Stokes–Leibenson Problem for Hele-Shaw Flows,” Patterns and Waves (Saint Petersburg, 2002), AkademPrint, St. Petersburg, 103–124 (2003).

12. A. S. Demidov and J.-P. Lohéac, "Numerical Scheme for Laplacian Growth Models Based on the Helmholtz–Kirchhoff Method," Analysis and Mathematical Physics, Trends Math., Birkhäuser, Basel, 107–114 (2009).
13. A. S. Demidov, J.-P. Lohéac, and V. Runge, "Problème de Cauchy pour l'approximation de Stokes–Leibenson d'une cellule de Hele–Shaw en coin," Comptes Rendus Mécanique **341** (11–12), 755–759 (2013).
14. A. S. Demidov and O. A. Vasilieva, "The Finite Point Model of the Stokes–Leibenson Problem for the Hele-Shaw Flow," Fundam. Prikl. Mat. **1**, 67–84 (1999).
15. J. Escher and G. Simonett, "Classical Solutions of Multidimensional Hele-Shaw Models," SIAM J. Math. Anal. **28**, 1028–1047 (1997).
16. F. D. Gakhov, *Boundary Value Problems* (Oxford, NY, Pergamon Press, 1966).
17. L. A. Galin, "Unsteady Filtration with a Free Surface," Dokl. Akad. Nauk SSSR **47**, 250–253 (1945).
18. B. Gustafsson, "Applications of Variational Inequalities to a Moving Boundary Problem for Hele-Shaw Flows," SIAM J. Math. Anal. **16** (2), 279–300 (1985).
19. B. Gustafsson and A. Vasil'ev, *Conformal and Potential Analysis in Hele-Shaw Cells* (Birkhäuser Verlag, Basel, 2006).
20. Yu. E. Hohlov and S. D. Howison, "On the Classification of Solutions to the Zero-Surface-Tension Model for Hele-Shaw Free Boundary Flows," Quart. Appl. Math. **51** (4), 777–789 (1993).
21. *Hele-Shaw Flows and Related Problems*, S. D. Howison and J. R. Ockendon, eds., European J. Appl. Math. **10** (6), 511–709 (1999).
22. H. Helmholtz, *Über discontinuirliche Flussigkeitsbewegungen* (Monatsber. Konigl.Akad.Wissenschaften, Berlin, 1868).
23. Yu. E. Khokhlov and S. D. Howison, "On the Classification of Solutions to the Zero-Surface-Tension Model for Hele-Shaw Free Boundary Flow," Quart. Appl. Math. **51** (4), 777–789 (1993).
24. G. Kirchhoff, *Zür Theorie freier Flussigkeitsstrahlen* (Borchardt's J., Bd. 70, 1869).
25. P. Ya. Kochina, *Selected Works. Hydrodynamics and Filtration Theory* (Nauka, Moscow, 1991) [in Russian].
26. P. P. Kufarev, "A Solution of the Boundary Problem for an Oil Well in a Circle," Doklady Akad. Nauk SSSR (N. S.) **60**, 1333–1334 (1948) [in Russian].
27. H. Lamb, *Hydrodynamics.* (Cambridge Univ. Press., 6th ed., Cambridge, 1932).
28. L. S. Leibenson, *Oil Producing Mechanics,* Part II (Moscow, Neftizdat, 1934) [in Russian].
29. A. M. Meirmanov and B. Zaltzman, "Global in Time Solution to the Hele- Shaw Problem with a Change of Topology," European J. Appl. Math. **13** (4), 431–447 (2002).
30. N. I. Muskhelishvili, *Some Basic Problems of the Mathematical Theory of Elasticity* [in Russian] (Leningrad, AN SSSR, 1949; Noordhoff Int. Publishing, Leiden, 1977).
31. J. R. Ockendon and S. D. Howison, "Kochina and Hele-Shaw in Modern Mathematics, Natural Sciences and Technology," J. Appl. Math. Mech. **66** (3), 505–512 (2002).
32. P. I. Plotnikov and V. N. Starovoïkov, "The Stefan Problem with Surface Tension as a Limit of the Phase Field Model," Differ. Uravn. **29** (3), 461–471 (1993) [Differ. Equ. **29** (3), 395–404 (1993)].
33. P. Ya. Polubarinova-Kochina, "On the Motion of the Oil Contour," Dokl. Akad. Nauk SSSR **47**, 254–257 (1945) [in Russian].
34. P. Ya. Polubarinova-Kochina, "Concerning Unsteady Motions in the Theory of Filtration," Prikl. Mat. Mech. **9**, 79–90 (1945) [in Russian].
35. M. Reissig and L. Wolfersdorf, "A Simplified Proof for a Moving Boundary Problem for Hele-Shaw Flows in the Plane," Ark. Mat. **31** (1), 101–116 (1993).
36. M. Sakai, "Regularity of a Boundary Having a Schwarz Function," Acta Math. **166**, 263–297 (1991).
37. M. Sakai, "Regularity of Free Boundaries in Two Dimensions," Ann. Sc. Norm. Super. Pisa Cl. Sci. **20**, 323–339 (1993).
38. H. S. Shapiro, *The Schwarz Function and Its Generalization to Higher Dimensions* (University of Arkansas lecture notes in the mathematical sciences, **9**, New-York, John Wiley & Sons Inc, 1992).
39. G. G. Stokes, *Mathematical Proof of the Identity of the Stream-Lines Obtained by Means of Viscous Film with Those of a Perfect Fluid Moving in Two Dimensions* (Brit. Ass. Rep., 143 (Papers, V, 278) 1898).
40. Yu. P. Vinogradov and P. P. Kufarev, "On a Problem of Filtration," Prikl. Mat. Mech. **12**, 181–198, (1948) [in Russian].